Critical size dependence of domain formation observed in coarse-grained simulations of bilayers composed of ternary lipid mixtures

George A. Pantelopulos,[1] Tetsuro Nagai,[2] Asanga Bandara,[1] Afra Panahi,[1] and John E. Straub[1,a)]

[1]*Department of Chemistry, Boston University, 590 Commonwealth Avenue, Boston, Massachusetts 02215, USA*
[2]*Department of Physics, Graduate School of Science, Nagoya University, Nagoya, Aichi 464-8602, Japan*

(Received 22 May 2017; accepted 19 July 2017; published online 1 September 2017)

Model cellular membranes are known to form micro- and macroscale lipid domains dependent on molecular composition. The formation of macroscopic lipid domains by lipid mixtures has been the subject of many simulation investigations. We present a critical study of system size impact on lipid domain phase separation into liquid-ordered and liquid-disordered macroscale domains in ternary lipid mixtures. In the popular di-C16:0 PC:di-C18:2 PC:cholesterol at 35:35:30 ratio mixture, we find systems with a minimum of 1480 lipids to be necessary for the formation of macroscopic phase separated domains and systems of 10 000 lipids to achieve structurally converged conformations similar to the thermodynamic limit. To understand these results and predict the behavior of any mixture forming two phases, we develop and investigate an analytical Flory-Huggins model which is recursively validated using simulation and experimental data. We find that micro- and macroscale domains can coexist in ternary mixtures. Additionally, we analyze the distributions of specific lipid-lipid interactions in each phase, characterizing domain structures proposed based on past experimental studies. These findings offer guidance in selecting appropriate system sizes for the study of phase separations and provide new insights into the nature of domain structure for a popular ternary lipid mixture. *Published by AIP Publishing.* [http://dx.doi.org/10.1063/1.4999709]

I. INTRODUCTION

Cellular membranes consist of a variety of types of lipids[1] combined with sterols and proteins.[2] The membrane environment is observed to be robust against local spatial disturbances and structural stress over the membrane surface yet dynamic in allowing lipid and protein diffusion and structural reorganization essential to cellular function.[3–5]

Lipid bilayer mixtures have been observed to form domains *in vitro*[6] and *in vivo*.[7,8] Lipids within a given domain are assumed to adopt one of many structural phases available to lipid bilayers,[9,10] constituting a thermodynamic model of "condensed complexes."[11] Lipid domains are observed to be micro- or macroscale depending on the lipid mixture, categorized as "type I" and "type II" mixtures by Feigenson.[12–14] The most widely discussed macroscale domain is known as a "lipid raft," characterized by high concentrations of cholesterol, sphingomyelin, and glycosylphosphatidylinositol-anchored proteins in a liquid-ordered phase (L_o),[15] conjectured to be critical to the structure and function of several membrane proteins.[16] Lipid domains are widely believed to be circular, formed via coarsening,[17–19] though the formation of circular domains via modulated phases has also been reported.[20]

Few component lipid bilayers have been designed as minimal models of biological membranes that retain characteristics believed to be essential to membrane function.[21–23] Investigations of model membranes using NMR spectroscopy,[24–27] fluorescence spectroscopy,[28–32] scattering techniques,[33–36] and microscopy techniques[28,37–40] have provided insight into the essential thermodynamic properties of lipid bilayers. Lattice models have provided insight into the fundamental thermodynamic driving forces leading to the phase behavior observed in experimental studies of ternary lipid mixtures.[41–46] This understanding of membrane structure and dynamics has been supplemented by increasingly detailed molecular simulation studies.[47–59] Taken together, these experimental, computational, and theoretical studies have supplied us with a fundamental understanding of the essential properties of membrane formation.[60–66]

In molecular dynamics simulations, periodic boundary conditions (PBCs) are used with the knowledge that observed thermodynamic and kinetic properties may depend on the finite size of the system.[67–69] In the case of lipid bilayer simulation, PBC effects were first investigated in the context of the spectrum of membrane surface undulations. Lindhal and Edholm found that the x- or y-edge length must be 20 nm or longer, and the system must be equilibrated for 10-100 ns to develop the longest wavelength undulatory modes required to fully characterize the bilayer surface. Klauda *et al.* found a strong dependence of lipid diffusion on the PBC size,[70] though Castro-Román *et al.* found the effect of PBC on single and multilamellar bilayer structures to be negligible.[71] Additionally Camley *et al.* have developed a Saffman-Delbrück

a)Electronic mail: straub@bu.edu

hydrodynamic model validated by all-atom and coarse-grained simulations, suggesting that lipid bilayer simulations must employ PBCs with near-100 nm edge lengths and thick hydration layers to capture essential bilayer structural fluctuations.[72] These studies suggest that PBCs strongly perturb lipid bilayer fluctuations and dynamics. In the case of domain formation by simple liquid mixtures, Scott *et al.*[73] have investigated the nature of system size and PBC effects, and Huang and Feigenson have investigated system size effects of phase separation in binary mixture lattice models.[74] However, the scaling of PBC effects observed in studies of liquid-liquid phase separation using molecular dynamics simulation does not appear to have been addressed in any context.

In this work, we perform molecular dynamics simulations and structural analysis of domain formation in the well-studied di-C16:0 PC (DPPC), di-C18:2 PC (DIPC), and cholesterol (CHOL) (35:35:30), "type II" ternary lipid bilayer mixture using MARTINI coarse-grained lipid models over a wide range of system sizes. Our analysis of domain formation as a function of system size suggests that systems with less than 1480 lipids may not form macroscale domains defined by a distinguishable interface. Moreover, the convergence of structural properties is found to require systems of 10 000 lipids or more. Additionally, via the microscopic structural analysis of *trans*-leaflet aggregates of L_o domain-forming lipids, we observe the coexistence of micro- and macroscopic ordered domains in systems of sufficient size. To describe the balance of finite size, composition, temperature, and interaction energy on phase separation and domain shape, we apply an analytical Flory-Huggins model parameterized using simulation data and interaction energies derived from experiment. These findings provide insight into the role of system size in determining the morphology and stability of domain formation in multicomponent lipid bilayers and guidance for future modeling studies. Additionally, this work suggests that finite size effects may be critical to the study of phase separation in other multi-component biological systems, such as the formation of the protein coronae, protein fibrils, endoplasmic granules, and vesicles.

II. MATERIALS AND METHODS

A. MD simulation setup

Fully atomistic simulations of lipid bilayer phase separation from random mixtures are not feasible with current enhanced sampling methods and computing hardware. As such, we employ the widely used MARTINI coarse-grained force field, which simplifies the energy landscape of the mixture, accelerates dynamics relative to atomistic models, and provides an order of magnitude gain in both computational efficiency for integration time step and number of particles (Fig. 1). While approximate, the MARTINI model has been shown to capture essential properties of a variety of thermodynamic phases, making it useful for understanding structural transitions in lipid membranes.[63,75]

The Melo *et al.* force field parameters were used for CHOL.[76] DPPC, DIPC, water, Na, and Cl were modeled using the MARTINI v2.0 parameters.[77] Approximately 24 effective solvent molecules per lipid molecule were used so as to fully solvate each lipid head group.[78] To avoid spontaneous freezing of water, 10% of the waters were modeled using antifreeze parameters. 150 mM NaCl salt was used to model a physiological salt concentration.

All ternary mixtures were prepared by the random placement of DPPC, DIPC, and CHOL on a square lattice bilayer with a layer of solvent using the insane.py tool.[79] The steepest descent minimization and MD were performed using the GROMACS 5.0.4 simulation suite.[80] Simulation parameters largely correspond to those of the "common" parameter set described by De Jong *et al.*[81] A time step of 20 fs using leapfrog integration with a 1.2 nm "group" neighbor list updated every 10 steps was used. Non-bonded interactions are handled using the Gromacs shifting function between 0.9-1.2 nm and 0.0-1.2 nm for Lennard-Jones and Coulomb interactions, respectively. The velocity-rescaling thermostat was used with a coupling time of 1 ps with 295 K temperature, and the semi isotropic Berendsen barostat was used with 1 atm pressure, a coupling time of 2 ps, and a compressibility of 3×10^{-4} bar^{-1}. Coordinates

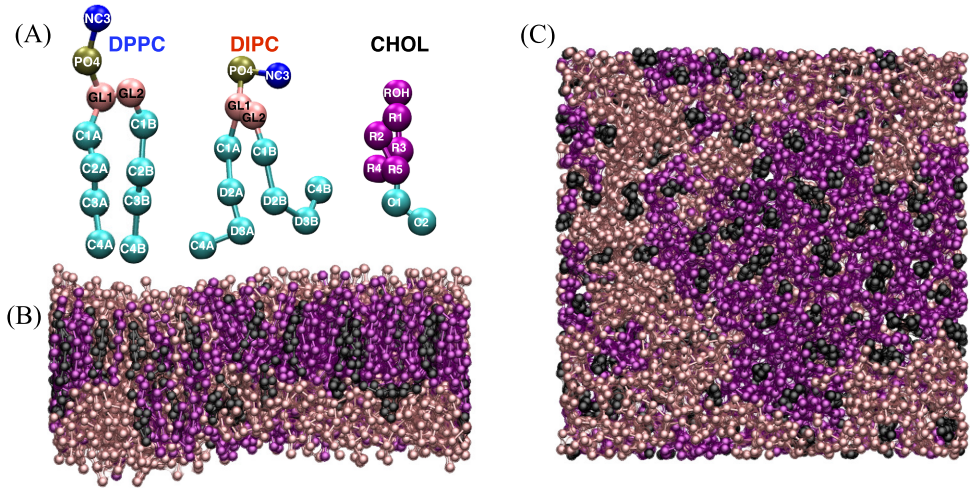

FIG. 1. (a) MARTINI model lipids and cholesterol with site labels. Slab (b) and top (c) views of N = 508 lipid membranes at 11 μs where DPPC, DIPC, and CHOL are pink, purple, and black, respectively.

and thermodynamic data were recorded in 1 ns time intervals.

B. Assignment of CHOL to leaflets

Due to rapid flip-flop between leaflets, CHOL molecules were assigned to a specific leaflet in each frame. Flip-flops of lipids other than CHOL were not observed. For each CHOL molecule, we assessed whether its head group is proximate to an upper or lower leaflet lipid head group and assigned it to the appropriate leaflet.

C. Analysis methods

Lipid mixing entropy (S_{mix}) was computed using nearest neighbors determined via Voronoi tessellations of lipid head groups. This method provides advantages over definitions of mixing entropies based on coarse-grained measurements of lipid composition within a space-fixed grid, the resolution of which influences the estimate of the mixing entropy.[82,83] The head groups, represented by the PO4 beads of DPPC and DIPC and the ROH bead of CHOL, were selected within each leaflet in each frame, from which a Voronoi tessellation was performed. The mixing entropy was determined based on the probability of contacts formed by the same lipid type (p_1) or different lipid type (p_2) as

$$S_{\mathrm{mix}} = -p_1 \log_2 p_1 - p_2 \log_2 p_2. \tag{1}$$

The Nelson-Halperin 2D bond-orientational order parameter (Ψ_6) was computed based on the carbon chain of each DPPC, DIPC, and CHOL. Positions of DPPC and DIPC chains were represented by C2A and C2B, and D2A and D2B beads, respectively. The CHOL chain was represented by the centroid of the R1, R2, R3, R4, and R5 beads. The six nearest neighbors (l) of each point (k) were found using the Cartesian coordinates of the k and l points fitted to a plane using their singular value decomposition prior to the measurement of Ψ_6. The reference vector, $\vec{r}$, was positioned at k, pointed along the x-axis, and was fitted to the same plane as the k and l points. Using the fitted plane, the bond-orientational order parameter was computed as

$$\Psi_6^k = \frac{1}{6} \sum_{l \in nn(k)}^{6} e^{i6\theta_{kl}}, \tag{2}$$

where θ_{kl} is the angle between the vector connecting l and k and the vector $\vec{r}$. Taking the absolute value, $|\Psi_6^k|$ gives us a measure of how "well-packed" a lipid tail is.

The liquid crystal order parameter (P_2) was measured using a vector between GL1-C4A and GL2-C4B beads for DPPC and DIPC and the z-axis as the director,

$$P_2 = 0.5(3\langle \cos^2(\theta_{ij}) \rangle - 1), \tag{3}$$

where θ_{ij} is the angle between the vector connecting the lipid tails and the director vector.

To identify intra-leaflet aggregates of DPPC and CHOL carbon chains, we performed a hierarchical distance-based geometric clustering analysis. We counted DPPC and CHOL carbon chains as being part of an aggregate if the C2A, C2B, or centroid of the R1, R2, R3, R4, and R5 beads were within 5.8 Å of any other beads. The inter-leaflet contacts were counted if the C4A, C4B (DPPC and DIPC), or C2 (CHOL) bead in the opposing leaflet were within 7.0 Å of any bead defining the aggregate. For the analysis of DIPC and CHOL aggregates, equivalent criterion for cluster identification was used except intra-leaflet aggregates which were identified using a 7.8 Å cutoff distance.

III. RESULTS AND DISCUSSION

A. Achieving structural and spatial equilibrium

To study the formation of phase separated domains, we employ a traditional "type II" mixture of DPPC, DIPC, and CHOL (35:35:30) previously investigated.[14,61–66,84–86] We performed coarse-grained MD simulations at 295 K initiated from a random spatial placement of lipids into a bilayer geometry for a wide range of system sizes. Five 11 μs trajectories were produced for bilayers composed of N = 240, 508, 1056, 2046, 3040, and 5406 molecules. 330 μs of sampling were accumulated for this study. These systems reach an apparent equilibrium in their structural properties by 6 μs, as measured by the time-dependence of the lipid mixing entropy (S_{mix}), the norm of their 2D bond-orientational order parameter ($|\Psi_6|$), and the liquid crystal order parameter (P_2) (Fig. 2). The time evolution of the instantaneous order parameters suggests that the system dynamics is essentially stationary after 6 μs.

B. Critical system size is required for phase separations

The average values of the three order parameters were computed as a function of system size using the dynamics in the observed stationary regime (Fig. 3). The average value of each order parameter displays a sigmoidal transition as a function of the log of system size, with a miscible state for small N and a phase separated state for large N. The average order parameters are observed to asymptotically converge at $N \approx 10\,000$, similar to that observed by Huang and Feigenson for binary lattice mixtures.[74] We identify a critical size (N_{c}) for each order parameter as the inflection point of the order parameter as a function of system size. We find that for the three order parameters employed, $N_{\mathrm{c}}^{S_{\mathrm{mix}}} = 994$, $N_{\mathrm{c}}^{P_2} = 870$, and $N_{\mathrm{c}}^{|\Psi_6|} = 1480$, close to $N_{\mathrm{c}} = 1000$ previously predicted by Huang and Feigenson.[74]

We observe that small equilibrated lipid bilayers up to $N = 1056$ do not form macroscopic phase separated domains spanning the system. Larger systems ($N \gtrsim 1480$) appear to form phase separated domains of size limited by the PBC employed. When $N \leq 1056$, liquid ordered domains do not span the system to form striped domains (Fig. 4). Based on these observations, we say that $N_{\mathrm{c}}^{|\Psi_6|} = 1480$ is the minimum system size required to simulate the formation of phase separated lipid domains. The separation of states by $|\Psi_6|$ is clear (Fig. S1 of the supplementary material) and the short correlation length of lipid tail orientational order [$\Psi_6(\boldsymbol{r})$] indicates that both phases retain characteristics of the liquid state (Fig. S2 of the supplementary material). Separation of states by P_2 is not as clearly visualized because this

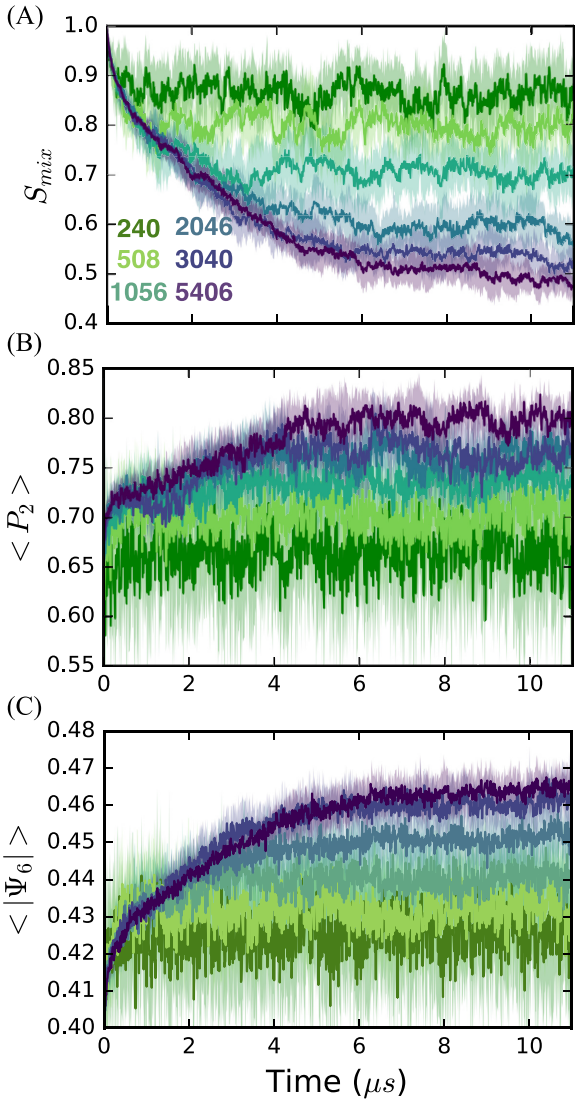

FIG. 2. Mean and standard deviations in (a) mixing entropy, (b) liquid crystal order, and (c) absolute value of 2D bond-orientational order averaged over five replicate trajectories.

is not measured for CHOL (Fig. S3 of the supplementary material).

C. Binary Flory-Huggins theory defines critical system size for domain formation

The phenomenon of phase separation in lipid bilayers has been considered using a variety of Flory-Huggins type models. Phase diagrams were computed for models of binary[41] and ternary[87] mixtures that included an order parameter based treatment of the liquid-gel melting transition. Additionally, a Flory-Huggins type model has been used to develop a theory of line tension in ternary lipid mixtures, finding the line tension to depend on the composition of the lipid mixture.[45] Finally, Radhakrishnan and McConnell developed a model for ternary lipid mixtures in which two components combine and interact with the third component.[42] While this last approach captures certain aspects of phase separation in ternary lipid mixtures noted in experiment, it fails to reproduce the more complex phase behavior captured by the more detailed models.

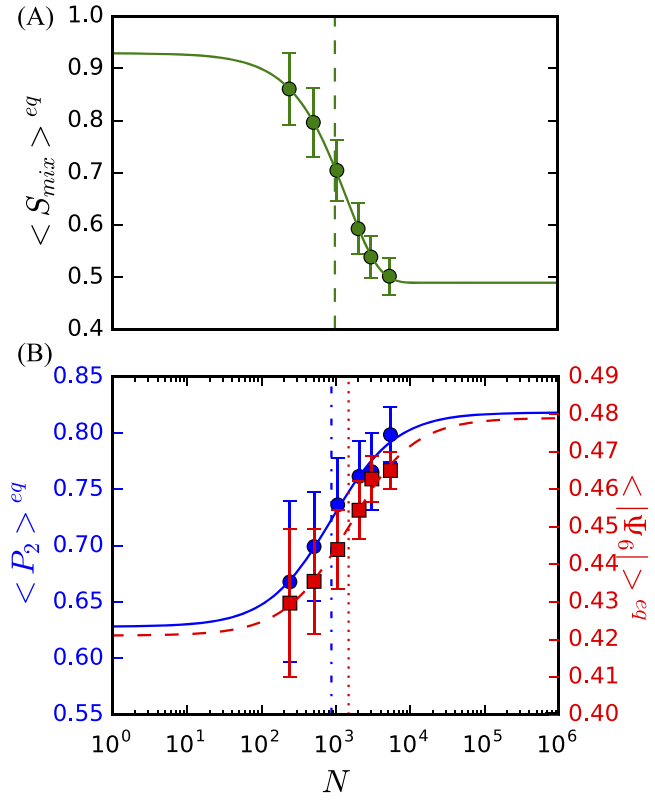

FIG. 3. Mean and standard deviations at equilibrium of (a) S_{mix} and (b) P_2 of DPPC (blue) and $|\Psi_6|$ of DPPC (dashed-red) averaged over five replicate trajectories. Inflection points are identified by dashed (S_{mix}), dashed-dotted (P_2), and dotted ($|\Psi_6|$) lines.

In this work, we employ a minimal model for the ternary lipid mixture in that it models the ternary mixtures in terms of two fluid components and bears resemblance to the model of McConnell and Vrljic[11] and to the original presentation of the theory.[88] It is used as a minimal model to provide insight into the importance of system size on phase separation and to determine the thermodynamic driving forces determining the minimum system size required to observe phase separated domains.

We define the free energy of a randomly mixed state (F_{mix}), a stripe phase separated state (F_{stripe}), and a dot-shaped (circular) phase separated state (F_{dot}) as

$$F_{\mathrm{mix}} = E_0 + Nz\chi x_{\mathrm{D}}(1-x_{\mathrm{D}}) + k_{\mathrm{B}}T\left(x_{\mathrm{D}}\ln x_{\mathrm{D}} + (1-x_{\mathrm{D}})\ln(1-x_{\mathrm{D}})\right), \quad (4)$$

$$F_{\mathrm{stripe}} = E_0 + 2\chi\sqrt{N}, \quad (5)$$

$$F_{\mathrm{dot}} = E_0 + 2\chi\sqrt{N}\sqrt{\pi x_{\mathrm{D}}}, \quad (6)$$

where N is the number of molecules in a monolayer, x_{D} is the mole fraction of molecules that form the liquid disordered phase ($\mathrm{L_d}$), ranging from 0 to 0.5, $x_{\mathrm{O}} = 1 - x_{\mathrm{D}}$ is the mole fraction of molecules that form the liquid ordered phase ($\mathrm{L_o}$), z is the coordination number of each molecule, E_0 is a constant for interaction energies, and $\chi = w_{\mathrm{DO}} - \frac{(w_{\mathrm{DD}}+w_{\mathrm{OO}})}{2}$ is a measure of the cost of forming an interaction between sites representing $\mathrm{L_o}$ and $\mathrm{L_d}$. w_{DD}, w_{OO}, and w_{DO} are bond energies discussed in detail in the supplementary material. When $\chi > 0$, it is possible for F_{stripe} or F_{dot} to reach a lower energy than F_{mixed}. The stripe phase is more stable than the dot phase for $1/\pi < x_{\mathrm{D}} < 1 - 1/\pi$.

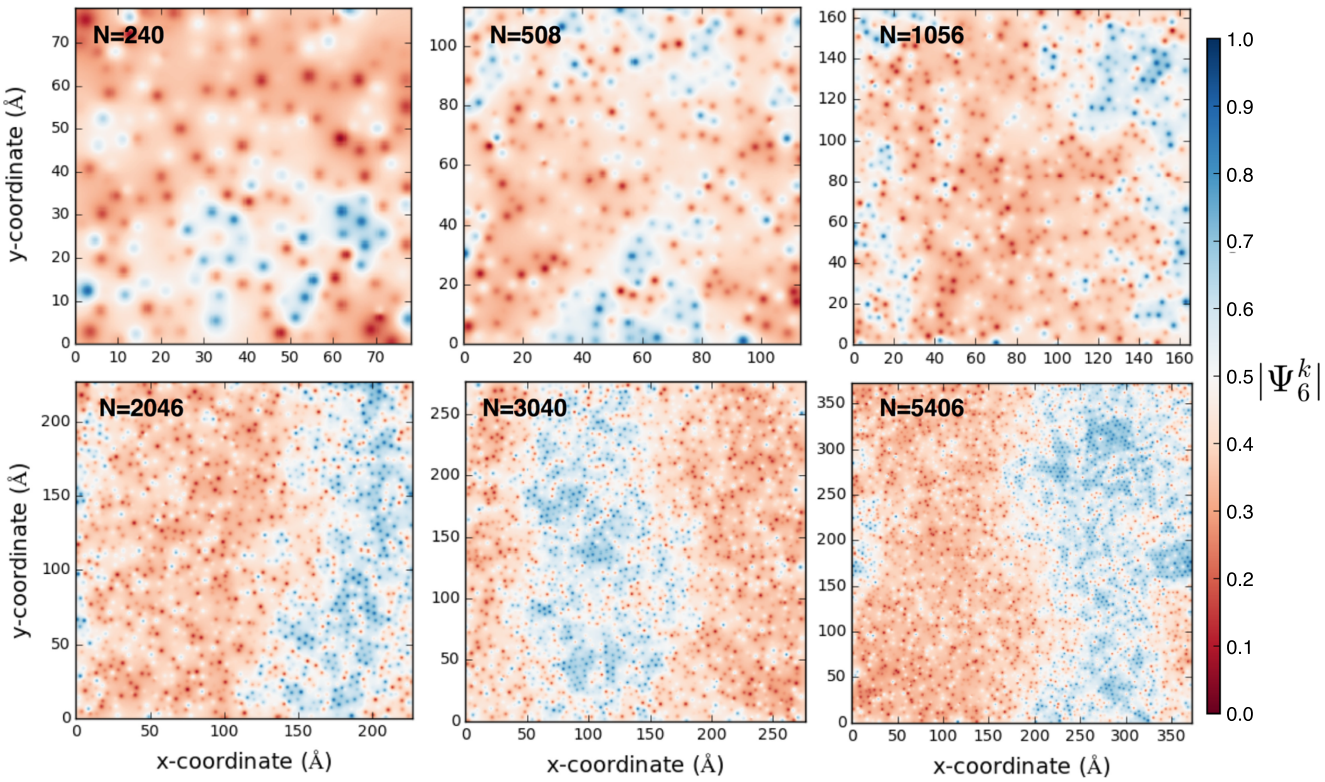

FIG. 4. Linearly interpolated measurements of absolute-valued 2D bond-orientational order parameter for one leaflet at 6 μs in different systems.

In our simulations, $x_D \approx 0.45$ (Table S2 of the supplementary material) and we observe the stripe phase, consistent with the predictions of the model. The crossover between miscible and immiscible states may happen as the number of lipids, N, in the system increases (Figs. 5 and 6).

This model enables prediction of N_c from experimentally determined χ, as well as the determination of χ values from N_c obtained by simulation [Fig. 6(b)]. The χ values corresponding to our simulations occur near the inflection point in $\chi(N)$, suggesting a sensitive dependence of N_c on χ. The χ values reported here are likely larger than other well-studied mixtures in experiment, such as DPPC, DIPC, and CHOL, due to substantial mismatch in degrees of tail saturation. This may explain the past difficulty in observing macroscopic phase separation of such mixtures in simulation studies.

There have been many previous studies of domain formation in ternary lipid mixtures using MARTINI as well as more fine-grained lipid force fields.[14,60–66,84–86,89–93] Some of the previous simulation work on this phenomenon employed system sizes substantially smaller than the critical minimum system size required for phase separation in this study.[62,65,66,90–92,94] As such, it is important to carefully

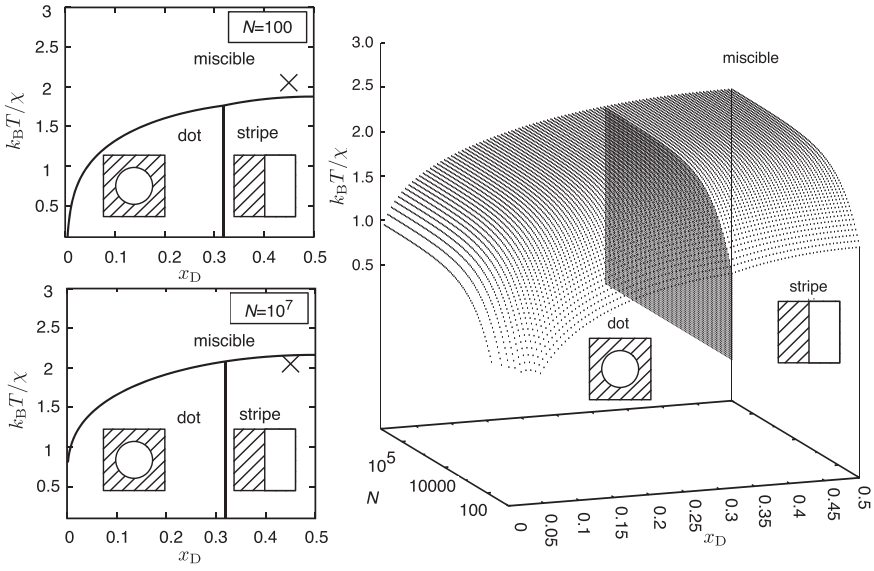

FIG. 5. Lowest free energy configurations found for the Flory-Huggins model of mixed, stripe, or dot states at T = 295 K and z = 6 (to approximate realistic lipid packing). The "X" depicts the state of the system considered in this work, which is predicted to be in the miscible state for N = 100 and stripe phase separated state for $N = 10^7$ taken to be the thermodynamic limit.

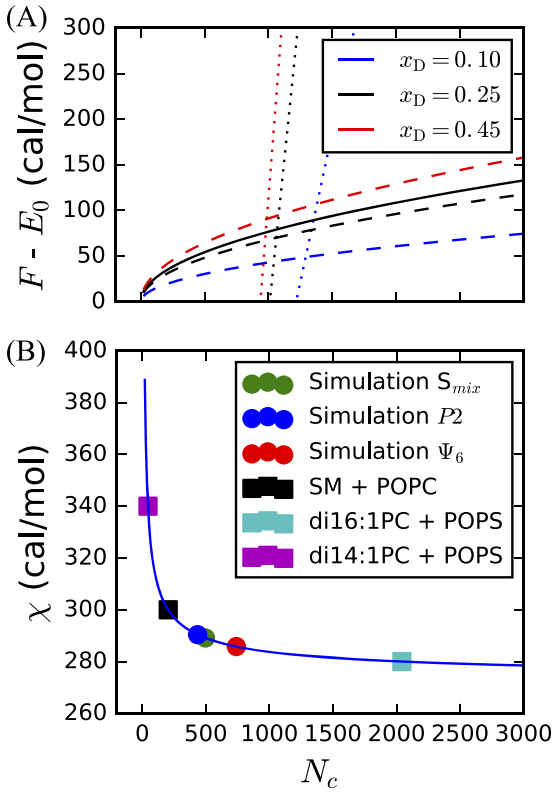

FIG. 6. We demonstrate the dependence of system size, N, on the mole fraction, x_D. (a) Free energies of mixed (dotted), stripe (solid), and dot (dashed) phases when χ = 2.90 cal/mol and T = 295 K. z = 6 to approximate realistic packing of lipids. (b) Solid line is the relation from the binary Flory-Huggins model [Eq. (S6) of the supplementary material] with x_D = 0.45, T = 295 K, and z = 6. Circles are placed on the curve at critical sizes (N_c) obtained from simulation, while squares are placed on the curve at χ values derived by Almeida.[95] χ and N_c values are tabulated along with corresponding line tensions in Table S3 of the supplementary material.

consider how PBC may have influenced observations of phase behavior in these previous studies.

D. Coexistence of micro- and macroscopic liquid ordered domains at equilibrium

To define domains of DPPC and CHOL aggregates, we geometrically cluster intra-leaflet DPPC and CHOL carbon chains (of number n) and identify inter-leaflet contacts with DPPC and CHOL (of number m) at equilibrium (see Sec. II for details). We count the occurrences of aggregates given (n, m). Through this analysis, we observe large separations between micro- and macroscopic domains once the system becomes large [Fig. 7(a) and Fig. S4 of the supplementary material]. Similar separation can be observed for DIPC and CHOL aggregates (Fig. S5 of the supplementary material). By analyzing the number of carbon chains not associated to the largest intraleaflet cluster, we also find that L_d domains in small systems exhibit substantial impurities while L_o domains are similarly pure at all system sizes (Fig. S6 of the supplementary material). Additionally, it appears that sampled values of n and m are linearly correlated, such that an aggregate of n intra-leaflet carbon chains will be in contact with a similar number of m inter-leaflet carbon chains. Analyzing aggregates of size n+m, we find microscopic domains as large as 250 carbon chains to be substantially ordered, forming a L_o domain [Fig. 7(b)]. This coexistence of micro- and macroscopic domains stands in contrast to the scenario in which ternary mixtures *only* form micro- (type I) or macro-domains (type II) as implied by Feigenson.[12–14] Similar observations have also been made based on binary mixture simulations of the Pink lattice model for lipid-lipid and lipid-protein mixtures, suggesting that microscopic phase separations can arise

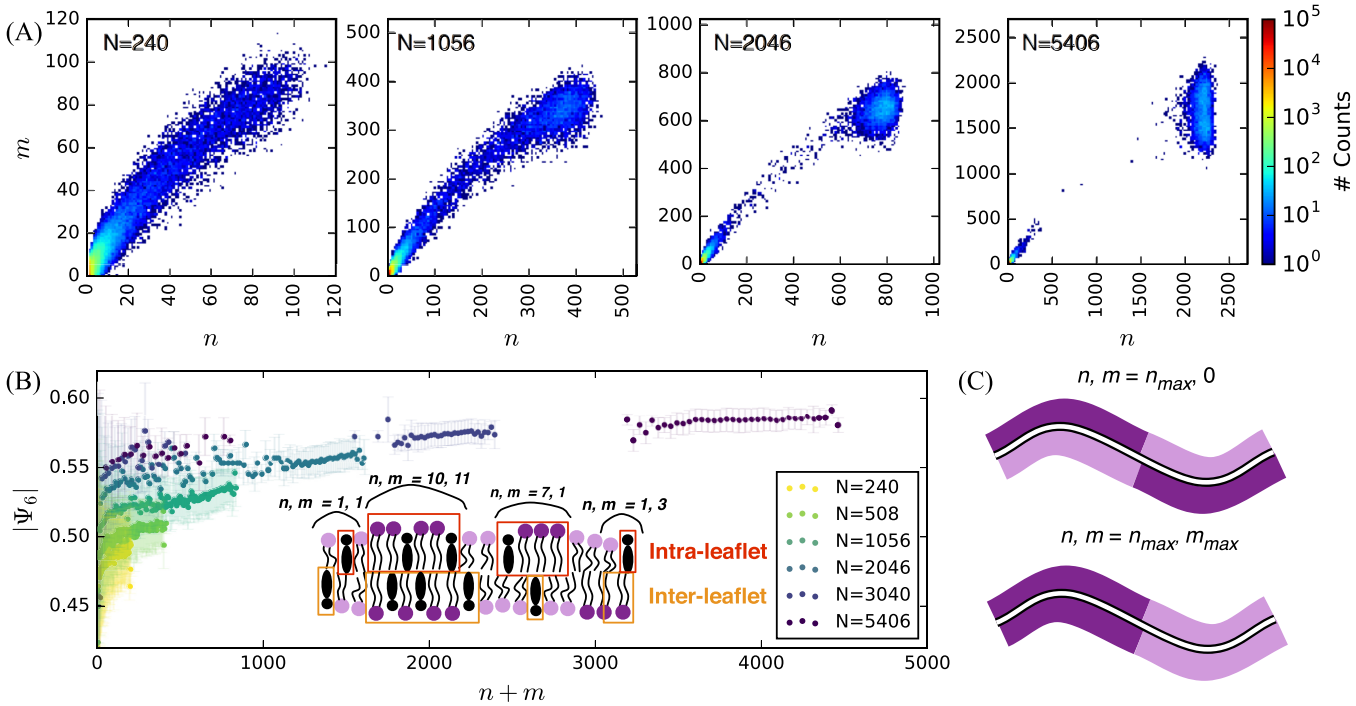

FIG. 7. (a) Counts of intra- (n) and inter-leaflet (m) carbon chains in DPPC-CHOL aggregates at equilibrium. (b) Mean and standard deviations of $|\Psi_6|$ as dependent on the size of DPPC-CHOL aggregates. Inset illustration describes aggregates in an example configuration. (c) Illustration of extreme cases of registration and anti-registration.

even when there is a vanishingly small amount of mismatching lipid.[96,97] Additionally, recent work by Javanainen *et al.* identifies the coexistence of microscopic L_o and L_d domains in all-atom simulations.[98]

E. Phases form unique complexes involving CHOL

To characterize the structure of lipids within the simulated L_o and L_d domains, we provide a critical comparison with the liquid condensed phase of DPPC and CHOL monolayers, analogous to the L_o phase. Kim *et al.* observed that liquid condensed domains in mixtures of DPPC and CHOL exhibit a high degree of bond-orientational order and a ratio of 6:1 DPPC:CHOL, consistent with the formation of a "tiled lattice" of cholesterol carbon chain surrounded by six DPPC carbon chains.[99] Consistent with this view, we observe substantial bond-orientational order which visually differentiates the L_o and L_d domains (Fig. 8).

Distributions of CHOL neighbors were evaluated via Voronoi tessellations, where DPPC:CHOL 6:1 ratio was found to be most prevalent in L_o domains (in which cholesterol only neighbors other cholesterol or DPPC). Approximately equal counts of 5:1 and 7:1 ratios were the next-most populous complexes (Fig. 9), the result of point defects in the membrane surface that facilitate bilayer undulations. These ratios are consistent with the spatial distributions observed by Kim *et al.*[99] in the liquid condensed phase. For smaller system sizes in the L_d phase, a 1:1 DIPC:CHOL ratio is found to be most prominent. As N increases, a second peak at 6:1 DPPC:CHOL develops (in the L_d phase), similar to that of DPPC:CHOL (in the L_o phase) (Fig. S7 of the supplementary material).

We note that the L_o phase exhibits the preferential formation of CHOL-CHOL dimers over monomers. This may be of interest in biological processes where CHOL-CHOL dimerization has been proposed to play a role. An example of this is the case of amyloid precursor protein C99-CHOL dimerization, which has been proposed to promote the formation of amyloidogenic Aβ protein implicated in Alzheimer's disease.[100,101] The competition between C99-C99, C99-CHOL, and CHOL-CHOL dimer formations appears to be critical to this process, although the exact mechanism is unclear.[102,103] Additionally, there is some evidence that γ-secretase, which cleaves C99 to form Aβ, is concentrated in L_o domains.[104] If CHOL recruits C99 to the L_o phase,[102] CHOL may form homodimers, freeing C99 to bind with γ-secretase, thus forming Aβ.

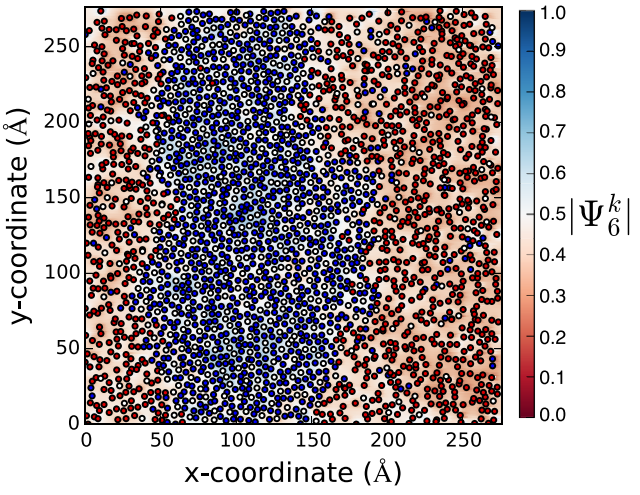

FIG. 8. Coordinates of DPPC (blue, C2A and C2B beads), DIPC (red, D2A and D2B beads), and CHOL (white, centroid of R1, R2, R3, R4, and R5 beads) in one leaflet at 6 μs for $N = 3040$. $|\Psi_6^k|$ values are linearly interpolated.

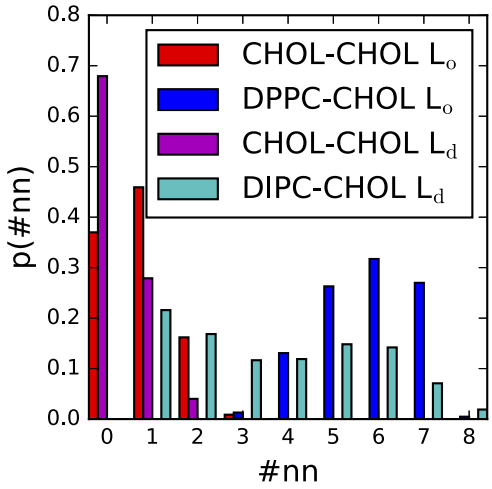

FIG. 9. Cholesterol nearest neighbor distributions computed using Voronoi tessellation analysis at apparent equilibrium for $N = 5406$. Cholesterol in L_o (L_d) domains are identified as cholesterols with no DIPC (DPPC) neighbors.

IV. CONCLUSION

In this work, we have investigated the effects of system size on macroscopic phase separation in lipid bilayers. We find that for the commonly investigated ternary lipid mixture, 35:35:30 DPPC:DIPC:CHOL, the system size must surpass 1480 lipids to observe the formation of stripe domains. This minimal number of lipids required for domain formation is likely to be similar or larger for other phase-separating mixtures, a conjecture supported by the predictions of a simple binary Flory-Huggins model. The binary Flory-Huggins model predicts a critical system size for domain formation and offers insight into the role of temperature, interaction energies, and system size in the domain formation process.

We have observed the coexistence of macro- and microscopic L_o domains within a "type II" macroscopic domain-forming mixture, in contrast to earlier observations. We have also quantified the effect of inter-leaflet contacts on the formation of domains. Additionally, we observe the spatial distribution of DPPC and CHOL observed in L_o domains to be consistent with the formation of 6:1 DPPC:CHOL complexes. Similar complexes are observed in the L_d phase formed by DIPC:CHOL in sufficiently large systems. Finally, we observe the preferential formation of CHOL-CHOL dimers over monomers in the L_o phase.

Taken together these observations demonstrate the importance of finite size effects in lipid phase separations. The importance of this observation is two-fold. There is a need to consider finite size effects when modeling phase behavior in lipid mixtures that is experimentally observed on the thermodynamic scale. In addition, when considering the

biological importance of phase separation, as in discussions of the existence and relevance of liquid-ordered "raft" domains, the observations made in this work suggest a lower limit on the size of domain formation in biological membrane.

SUPPLEMENTARY MATERIAL

See supplementary material for system composition and dimensions, molar fractions (x_D), interaction penalties (χ), line tensions (λ), critical system sizes (N_c), histograms of liquid crystal (P_2), and absolute value of bond-orientational order parameters ($|\Psi_6|$) at equilibrium, visualizations of Ψ_6^k and P_2, distributions of intra- (n) and inter-leaflet (m) clusters of DPPC-CHOL and DIPC-CHOL at equilibrium, L_o and L_d domain impurities at equilibrium, and CHOL-lipid nearest neighbor distributions at equilibrium. Additionally, it describes the binary Flory-Huggins model in detail.

ACKNOWLEDGMENTS

G.A.P. thanks the NSF GRFP for support under NSF Grant No. DGE-1247312. T.N. gratefully acknowledges the support by a Grant-in-Aid for Young Scientists (B) under Grant No. 26790083. J.E.S. is grateful to the Japan Society for the Promotion of Science (JSPS) Invitation Fellowship (Grant No. L13523) and BRIDGE Fellowship (Grant No. BR160401) during his stay at Nagoya University and thanks Professor Y. Okamoto for helpful discussions. We also acknowledge the generous support of the National Science Foundation (Grant No. CHE-1362524) and the National Institutes of Health (Grant No. R01 GM107703).

[1] M. Carquin, L. D'Auria, H. Pollet, E. R. Bongarzone, and D. Tyteca, Prog. Lipid Res. **62**, 1 (2016).
[2] G. L. Nicolson, "The Fluid—Mosaic model of membrane structure: Still relevant to understanding the structure, function and dynamics of biological membranes after more than 40 years," Biochim. Biophys. Acta, Biomembr. **1838**, 1451 (2014).
[3] J. L. Sampaio, M. J. Gerl, C. Klose, C. S. Ejsing, H. Beug, K. Simons, and A. Shevchenko, Proc. Natl. Acad. Sci. U. S. A. **108**, 1903 (2011).
[4] H. Giang, R. Shlomovitz, and M. Schick, Essays Biochem. **57**, 21 (2015).
[5] A.-E. Saliba, I. Vonkova, S. Deghou, S. Ceschia, C. Tischer, K. G. Kugler, P. Bork, J. Ellenberg, and A.-C. Gavin, Nat. Protoc. **11**, 1021 (2016).
[6] M. Edidin, Curr. Opin. Struct. Biol. **7**, 528 (1997).
[7] C. Eggeling, C. Ringemann, R. Medda, G. Schwarzmann, K. Sandhoff, S. Polyakova, V. N. Belov, B. Hein, C. von Middendorff, A. Schönle, and S. W. Hell, Nature **457**, 1159 (2009).
[8] A. Toulmay and W. A. Prinz, J. Cell Biol. **202**, 35 (2013).
[9] S. Sonnino and A. Prinetti, Curr. Med. Chem. **20**, 4 (2012).
[10] R. Koynova and M. Caffrey, Biochim. Biophys. Acta, Rev. Biomembr. **1376**, 91 (1998).
[11] H. M. McConnell and M. Vrljic, Annu. Rev. Biophys. Biomol. Struct. **32**, 469 (2003).
[12] G. W. G. Feigenson, Annu. Rev. Biophys. Biomol. Struct. **36**, 63 (2007).
[13] G. W. Feigenson, Biochim. Biophys. Acta, Biomembr. **1788**, 47 (2009).
[14] D. G. Ackerman and G. W. Feigenson, J. Phys. Chem. B **119**, 4240 (2015).
[15] D. Lingwood and K. Simons, Science **327**, 46 (2010).
[16] K. Simons and E. Ikonen, Nature **387**, 569 (1997).
[17] A. J. Bray, Adv. Phys. **43**, 357 (1994).
[18] M. Yanagisawa, M. Imai, T. Masui, S. Komura, and T. Ohta, Biophys. J. **92**, 115 (2007).
[19] I. Levental and S. Veatch, J. Mol. Biol. **428**, 4749 (2016).
[20] P. Pathak and E. London, Biophys. J. **109**, 1630 (2015).
[21] M. Edidin, Nat. Rev. Mol. Cell Biol. **4**, 414 (2003).
[22] K. Simons and W. L. C. Vaz, Annu. Rev. Biophys. Biomol. Struct. **33**, 269 (2004).
[23] Y.-H. M. Chan and S. G. Boxer, Curr. Opin. Chem. Biol. **11**, 581 (2007).
[24] J. Seelig, Q. Rev. Biophys. **10**, 353 (1977).
[25] J. H. Davis, Biochim. Biophys. Acta, Rev. Biomembr **737**, 117 (1983).
[26] A. Grélard, C. Loudet, A. Diller, and E. J. Dufourc, "NMR spectroscopy of lipid bilayers," in *Membrane Protein Structure Determination: Methods and Protocols*, edited by J.-J. Lacapére (Humana Press, Totowa, NJ, 2010), pp. 341–359.
[27] S. J. Opella, Acc. Chem. Res. **46**, 2145 (2013).
[28] S. L. Veatch and S. L. Keller, Biophys. J. **85**, 3074 (2003).
[29] S. L. Veatch, P. Cicuta, P. Sengupta, A. Honerkamp-Smith, D. Holowka, and B. Baird, ACS Chem. Biol. **3**, 287 (2008).
[30] A. S. Klymchenko and R. Kreder, Chem. Biol. **21**, 97 (2014).
[31] H. Basit, S. G. Lopez, and T. E. Keyes, Methods **68**, 286 (2014).
[32] E. Hermann, J. Ries, and A. J. García-Sáez, "Scanning fluorescence correlation spectroscopy on biomembranes," in *Methods in Membrane Lipids*, edited by D. M. Owen (Springer, New York, NY, 2015), pp. 181–197.
[33] J. F. Nagle and S. Tristram-Nagle, Biochim. Biophys. Acta **1469**, 159 (2000).
[34] G. Pabst, N. Kučerka, M.-P. Nieh, M. C. Rheinstädter, and J. Katsaras, Chem. Phys. Lipids **163**, 460 (2010).
[35] J. F. Nagle, Faraday Discuss. **161**, 11 (2013).
[36] D. Marquardt, B. Geier, and G. Pabst, Membranes **5**, 180 (2015).
[37] D. J. Müller and K. Anderson, Trends Biotechnol. **20**, S45 (2002).
[38] R. Dimova, S. Aranda, N. Bezlyepkina, V. Nikolov, K. A. Riske, and R. Lipowsky, J. Phys.: Condens. Matter **18**, S1151 (2006).
[39] J. Andrecka, K. M. Spillane, J. Ortega-Arroyo, and P. Kukura, ACS Nano **7**, 10662 (2013).
[40] L. A. Bagatolli and D. Needham, Chem. Phys. Lipids **181**, 99 (2014).
[41] S. Komura, H. Shirotori, P. D. Olmsted, and D. Andelman, Europhys. Lett. **67**, 321 (2004).
[42] A. Radhakrishnan and H. McConnell, Proc. Natl. Acad. Sci. U. S. A. **102**, 12662 (2005).
[43] P. W. Tumaneng, S. A. Pandit, G. Zhao, and H. L. Scott, Phys. Rev. E: Stat., Nonlinear, Soft Matter Phys. **83**, 031925 (2011).
[44] P. W. Tumaneng, S. A. Pandit, G. Zhao, and H. L. Scott, J. Chem. Phys. **132**, 065104 (2010).
[45] T. Idema, J. M. J. Van Leeuwen, and C. Storm, Phys. Rev. E: Stat., Nonlinear, Soft Matter Phys. **80**, 04192 (2009).
[46] R. Reigada, J. Buceta, J. Gómez, F. Sagués, and K. Lindenberg, J. Chem. Phys. **128**, 025102 (2008).
[47] R. W. Pastor, Curr. Opin. Struct. Biol. **4**, 486 (1994).
[48] D. J. Tobias, K. Tu, and M. L. Klein, Curr. Opin. Colloid Interface Sci. **2**, 15 (1997).
[49] D. P. Tieleman, S. J. Marrink, and H. J. C. Berendsen, Biochim. Biophys. Acta, Rev. Biomembr **1331**, 235 (1997).
[50] E. Jakobsson, Trends Biochem. Sci. **22**, 339 (1997).
[51] L. Forrest, Curr. Opin. Struct. Biol. **10**, 174 (2000).
[52] R. W. Pastor, R. M. Venable, and S. E. Feller, Acc. Chem. Res. **35**, 438 (2002).
[53] S. J. Marrink, A. H. de Vries, and D. P. Tieleman, Biochim. Biophys. Acta, Biomembr. **1788**, 149 (2009).
[54] W. F. D. Bennett and D. P. Tieleman, Biochim. Biophys. Acta, Biomembr. **1828**, 1765 (2013).
[55] X. Zhuang, J. R. Makover, W. Im, and J. B. Klauda, Biochim. Biophys. Acta, Biomembr. **1838**, 2520 (2014).
[56] O. H. S. Ollila and G. Pabst, Biochim. Biophys. Acta, Biomembr. **1858**, 2512 (2016).
[57] T. Mori, N. Miyashita, W. Im, M. Feig, and Y. Sugita, Biochim. Biophys. Acta, Biomembr. **1858**, 1635 (2016).
[58] A. Bandara, A. Panahi, G. A. Pantelopulos, and J. E. Straub, J. Comput. Chem. **38**, 1479 (2017).
[59] D. S. Patel, S. Park, E. L. Wu, M. S. Yeom, G. Widmalm, J. B. Klauda, and W. Im, Biophys. J. **111**, 1987 (2016).
[60] S. J. Marrink, J. Risselada, and A. E. Mark, Chem. Phys. Lipids **135**, 223 (2005).
[61] L. V. Schafer, D. H. de Jong, A. Holt, A. J. Rzepiela, A. H. de Vries, B. Poolman, J. A. Killian, and S. J. Marrink, Proc. Natl. Acad. Sci. U. S. A. **108**, 1343 (2011).
[62] J. D. Perlmutter and J. N. Sachs, J. Am. Chem. Soc. **133**, 6563 (2011).
[63] S. L. Duncan, I. S. Dalal, and R. G. Larson, Biochim. Biophys. Acta, Biomembr. **1808**, 2450 (2011).
[64] J. Domański, S. J. Marrink, and L. V. Schäfer, Biochim. Biophys. Acta, Biomembr. **1818**, 984 (2012).
[65] D. Hakobyan and A. Heuer, J. Phys. Chem. B **117**, 3841 (2013).

[66]R. S. Davis, P. B. Sunil Kumar, M. M. Sperotto, and M. Laradji, J. Phys. Chem. B **117**, 4072 (2013).
[67]I.-C. Yeh, J. Phys. Chem. B **108**, 15873 (2004).
[68]K. Takemura and A. Kitao, J. Phys. Chem. B **111**, 11870 (2007).
[69]B. Chandramouli, C. Zazza, G. Mancini, and G. Brancato, J. Phys. Chem. A **119**, 5465 (2015).
[70]J. B. Klauda, B. R. Brooks, and R. W. Pastor, J. Chem. Phys. **125**, 144710 (2006).
[71]F. Castro-Román, R. W. Benz, S. H. White, and D. J. Tobias, J. Phys. Chem. B **110**, 24157 (2006).
[72]B. A. Camley, M. G. Lerner, R. W. Pastor, and F. L. H. Brown, J. Chem. Phys. **143**, 243113 (2015).
[73]W. Scott, F. Müller-Plathe, and W. F. V. Gunsteren, Mol. Phys. **82**, 1049 (1994).
[74]J. Huang and G. W. Feigenson, Biophys. J. **65**, 1788 (1993).
[75]T. Nagai, R. Ueoka, and Y. Okamoto, J. Phys. Soc. Jpn. **81**, 024002 (2012).
[76]M. N. Melo, H. I. Ingólfsson, and S. J. Marrink, J. Chem. Phys. **143**, 243152 (2015).
[77]S. J. Marrink, H. J. Risselada, S. Yefimov, D. P. Tieleman, and A. H. D. Vries, J. Phys. Chem. B **111**, 7812 (2007).
[78]S. V. Dvinskikh, V. Castro, and D. Sandström, Phys. Chem. Chem. Phys. **7**, 3255 (2005).
[79]T. A. Wassenaar, H. I. Ingólfsson, R. A. Böckmann, D. P. Tieleman, and S. J. Marrink, J. Chem. Theory Comput. **11**, 2144 (2015).
[80]S. Pronk, S. Páll, R. Schulz, P. Larsson, P. Bjelkmar, R. Apostolov, M. R. Shirts, J. C. Smith, P. M. Kasson, D. Van Der Spoel, B. Hess, and E. Lindahl, Bioinformatics **29**, 845 (2013).
[81]D. H. De Jong, S. Baoukina, H. I. Ingólfsson, and S. J. Marrink, Comput. Phys. Commun. **199**, 1 (2016).
[82]M. Camesasca, M. Kaufman, and I. Manas-Zloczower, Macromol. Theory Simul. **15**, 595 (2006).
[83]G. B. Brandani, M. Schor, C. E. MacPhee, H. Grubmüller, U. Zachariae, and D. Marenduzzo, PLoS ONE **8**, e65617 (2013).
[84]Q. Liang, Q.-Y. Wu, and Z.-Y. Wang, J. Chem. Phys. **141**, 074702 (2014).
[85]D. L. Parton, A. Tek, M. Baaden, and M. S. P. Sansom, PLoS Comput. Biol. **9**, e1003034 (2013).
[86]C. Rosetti and C. Pastorino, J. Phys. Chem. B **115**, 1002 (2011).
[87]S. Komura, H. Shirotori, and P. D. Olmsted, J. Phys.: Condens. Matter **17**, S2951 (2005).
[88]P. J. Flory, J. Chem. Phys. **10**, 51 (1942).
[89]E. M. Curtis, X. Xiao, S. Sofou, and C. K. Hall, Langmuir **31**, 1086 (2015).
[90]I. Basu and C. Mukhopadhyay, Phys. Chem. Chem. Phys. **17**, 17130 (2015).
[91]C. Hong, D. P. Tieleman, and Y. Wang, Langmuir **30**, 11993 (2014).
[92]C. M. MacDermaid, H. K. Kashyap, R. H. DeVane, W. Shinoda, J. B. Klauda, M. L. Klein, and G. Fiorin, J. Chem. Phys. **143**, 243144 (2015).
[93]C. Rosetti and C. Pastorino, J. Phys. Chem. B **116**, 3525 (2012).
[94]A. J. Sodt, M. L. Sandar, K. Gawrisch, R. W. Pastor, and E. Lyman, J. Am. Chem. Soc. **136**, 725 (2014).
[95]P. F. F. Almeida, Biochim. Biophys. Acta, Biomembr. **1788**, 72 (2009).
[96]Z. Zhang, M. M. Sperotto, M. J. Zuckermann, and O. G. Mouritsen, Biochim. Biophys. Acta, Biomembr. **1147**, 154 (1993).
[97]J. Risbo, M. M. Sperotto, and O. G. Mouritsen, J. Chem. Phys. **103**, 3643 (1995).
[98]M. Javanainen, H. Martinez-Seara, and I. Vattulainen, Sci. Rep. **7**, 1143 (2017).
[99]K. Kim, S. Q. Choi, Z. A. Zell, T. M. Squires, and J. A. Zasadzinski, Proc. Natl. Acad. Sci. U. S. A. **110**, E3054 (2013).
[100]Y. Song, K. F. Mittendorf, Z. Lu, and C. R. Sanders, J. Am. Chem. Soc. **136**, 4093 (2014).
[101]E. Winkler, A. Julius, H. Steiner, and D. Langosch, Biochemistry **54**, 6149 (2015).
[102]Y. Song, E. J. Hustedt, S. Brandon, and C. R. Sanders, Biochemistry **52**, 5051 (2013).
[103]A. Panahi, A. Bandara, G. A. Pantelopulos, L. Dominguez, and J. E. Straub, J. Phys. Chem. Lett. **7**, 3535 (2016).
[104]R. Ehehalt, P. Keller, C. Haass, C. Thiele, and K. Simons, J. Cell Biol. **160**, 113 (2003).